

Z. F. Zhang^{1,2}, Z. G. Wang¹

¹Shenyang National Laboratory for Material Science, Institute of Metal Research, Chinese Academy of Sciences, Shenyang, P. R. China

²Institute for Metallic Materials, Dresden, Germany

Comparison of fatigue lives between grain boundaries and component single crystals of copper bicrystals

Fatigue lives of grain boundaries (GBs) and component crystals were measured by using [123]/[335] and [5 9 13]/[579] Cu bicrystals with a perpendicular GB at room temperature in air. The results show that the GBs were always the preferential sites for fatigue crack initiation and propagation in the two groups of bicrystals under cyclic tension-tension loading as well as push-pull straining control. When an [123]/[335] bicrystal with reduced section area was tested by cyclic tension-tension loading, the [335] component crystal always had a relatively higher fatigue life than the [123] component crystal. As a result, the fatigue life increased in the order of GB, [123] and [335] component crystals. When the two groups of bicrystals were subjected to cyclic push-pull straining, the GB of the [5 9 13]/[579] bicrystal showed a higher fatigue life than that of the [123]/[335] bicrystal, which was suggested to be partially attributed to the difference in the component crystal orientations in the two bicrystals. By using scanning electron microscopy and electron channeling contrast techniques, the fatigue damage features on the surfaces and fatigue fractography were examined. Based on the present results, the fatigue cracking mechanisms along GBs and persistent slip bands in Cu bicrystals are discussed.

Keywords: Bicrystals; Grain boundaries; Persistent slip bands; Fatigue life; Fatigue cracking; Fractography

1 Introduction

The control of properties, the improvement in performance or development of a new property can be achieved by adjusting the microstructures of materials. Grain boundaries (GBs) and phase boundaries (PBs) are important elements in the microstructure of most engineering materials. Therefore, the role of GBs in materials development has been given much attention by many investigators [1–3]. Generally, the GB properties strongly depend on their types and structures; accordingly, the bulk properties of polycrystals can be regarded as the total effect of various types of GBs. Fatigue cracking along GBs in polycrystals [4–9] and various bicrystals [10–20] has been investigated systematically. Several GB cracking models have been proposed to explain intergranular fatigue failure of polycrystals [4–6, 8, 10].

In our recent studies, fatigue-cracking phenomena along GBs had been observed and investigated in different Cu bi-

crystals [13–20]. An important finding is that a fatigue crack always tends to nucleate along the GBs of the Cu bicrystals no matter whether the GBs were perpendicular, parallel or tilted to the stress axis. It is of special importance for the control and design of high-performance polycrystalline materials when the GB cracking mechanism is clarified. On the other hand, except for the GB structure, the component crystals with different orientations can also play an important role in fatigue life of GBs. However, as far as we are aware, there is no quantitative knowledge about the fatigue life of GBs yet. As we know, for Cu bicrystals with a parallel GB, the final fatigue failure could not take place along the GB plane. Therefore, in the present work, we will employ Cu bicrystals with a perpendicular GB to compare their fatigue lives under different loading modes for a better understanding of the fatigue damage mechanism induced by slip bands and GBs.

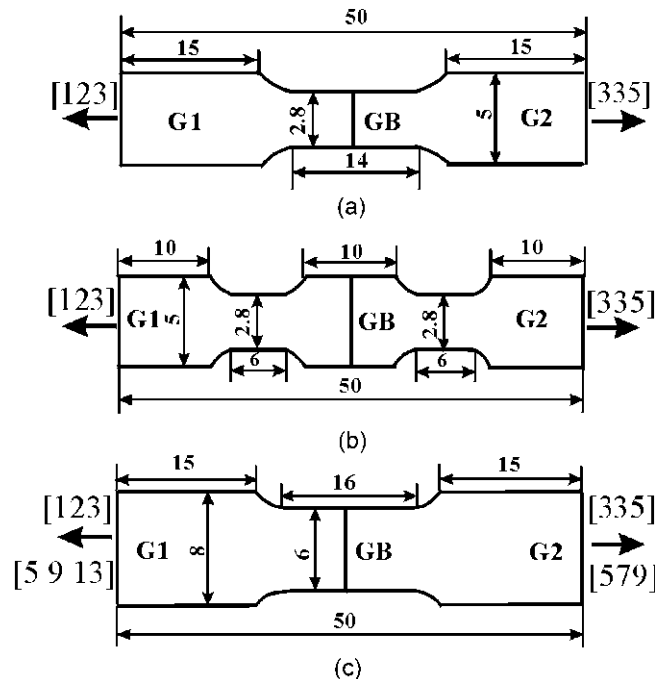


Fig. 1. Fatigue specimens used to determine the fatigue lives of (a) the GB of [123]/[335] bicrystals; (b) [123] and [335] component crystals under cyclic tension-tension loading and (c) GBs of the [123]/[335] and [5 9 13]/[579] bicrystals under cyclic push-pull straining control. The thickness of the bicrystals is always 3 mm. The number for the dimensions is given in millimeter.

2 Experimental procedure

Bicrystals with the size of $200\text{ mm} \times 50\text{ mm} \times 10\text{ mm}$ were grown from oxygen-free high-conductivity Cu of 99.999% purity by the Bridgman method in a horizontal furnace. The fatigue specimens with a GB plane perpendicular to the stress axis were spark-machined from the bicrystal plates, as shown in Figs. 1a and b. By the Laue back-reflection method, the stress axis orientations of two component crystals were determined as [123] and [335], respectively, which orient for typical single- and double-slip. Before the tests, all the bicrystal specimens were electrolytically polished to produce a strain-free surface for the microscopic observations. To compare the strength between GBs and their component crystals, firstly, several [123]/[335] bicrystal samples (Fig. 1a) were applied to tensile load until fracture on a Shimadzu servo-hydraulic testing machine at room temperature in air. After that, cyclic tension-tension tests of the specimens (a) and (b) were performed under constant load control. The stress ratio was about 0.1 and a triangle wave with a frequency of 10 Hz was used.

It should be pointed out that the specimen in Fig. 1a with a uniform section area was used to determine the GB fatigue life of [123]/[335] bicrystals. The specimen with double-reduced sections (Fig. 1b) was used to measure the fatigue lives of the component crystals. After the failure of one crystal, the fractured specimen (b) was further subjected to cyclic loading in order to measure the residual fatigue life of the other crystal under the same cyclic load.

Besides, to compare the difference in the fatigue lives of GBs in different bicrystals, [123]/[335] and [5 9 13]/[579] Cu bicrystal samples were prepared, as shown in Fig. 1c. Cyclic deformation was controlled under symmetrical push-pull strain with a triangle wave of 1 Hz, as reported previously [20]. When the bicrystal specimen fractured along the GB, the cyclic number to failure was regarded as the fatigue life of the GB.

Then, the specimen surface and fracture were observed by scanning electron microscopy (SEM) to examine the fatigue-cracking process. To reveal the GB cracking mechanism well, instead of the commonly used transmission electron microscopy (TEM) technique, an electron channeling contrast (ECC) technique in scanning electron microscopy (SEM) was adopted for observing the dislocation patterns in the present study. In comparison with TEM, the SEM-ECC technique has been reported to have many attractive features [21–24]. Especially, it is extremely suitable for studying the dislocation arrangements over a large specimen area and at some special sites, for example, the vicinity of GBs [19, 20, 25, 26], deformation bands [27, 28] and cracks [9, 28, 29]. Furthermore, the dependence of intergranular fatigue cracking on the interactions of persistent slip bands (PSBs) with GBs can be clearly exposed with the help of the SEM-ECC technique.

3 Results and discussion

3.1 Comparison of fatigue lives between GBs and component crystals

Prior to the fatigue test, tensile deformation was applied to the [123]/[335] bicrystal sample of Fig. 1a. It was found that the [123] crystal always displayed serious plastic deformation, then necked, and in the end, transgranular fracture occurred. However, the [335] crystal and the GB did not display very serious plastic deformation after fracture of the [123] crystal. This indicates that the GB and the [335] crystal in the [123]/[335] bicrystal possess a relatively higher strength than the [123] crystal under tensile loading. When the [123]/[335] bicrystal specimen of Fig. 1a was subjected to cyclic tension-tension loading, however, the GB was always the preferential failure site. When the [123]/[335] bicrystal specimen with reduced areas (Fig. 1b) was subjected to cyclic tension-tension loading, transgranular fracture always occurred along the [123] crystal. By applying the same cyclic tension-tension load to the fractured

specimen, then necked, and in the end, transgranular fracture occurred. However, the [335] crystal and the GB did not display very serious plastic deformation after fracture of the [123] crystal. This indicates that the GB and the [335] crystal in the [123]/[335] bicrystal possess a relatively higher strength than the [123] crystal under tensile loading. When the [123]/[335] bicrystal specimen of Fig. 1a was subjected to cyclic tension-tension loading, however, the GB was always the preferential failure site. When the [123]/[335] bicrystal specimen with reduced areas (Fig. 1b) was subjected to cyclic tension-tension loading, transgranular fracture always occurred along the [123] crystal. By applying the same cyclic tension-tension load to the fractured

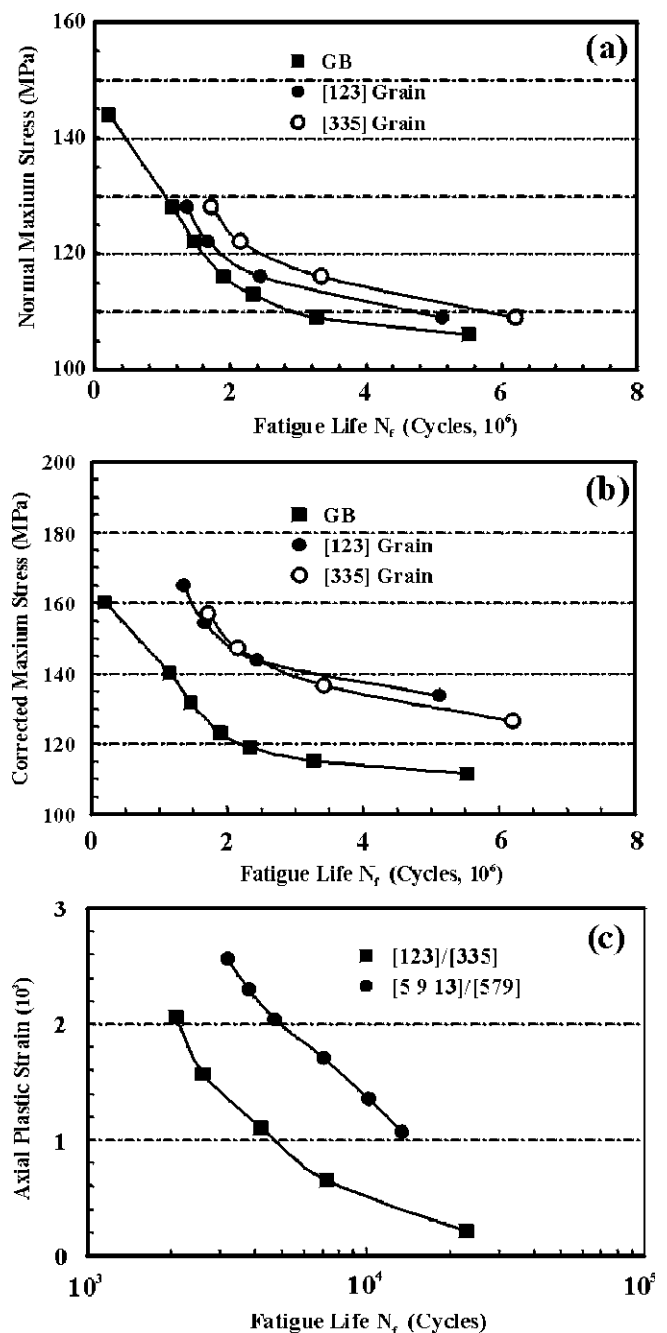


Fig. 2. (a, b) Fatigue life curves of the GB, and the [123] and [335] component crystals in a [123]/[335] bicrystal under cyclic tension-tension loading. (c) GB fatigue life curves of the [123]/[335] and [5 9 13]/[579] bicrystals under cyclic push-pull straining.

Table 1. Schmid factor of primary slip systems of the four component crystals in [123]/[335] and [5 9 13]/[579] Cu bicrystals.

Orientation	[123]	[335]	[5 9 13]	[579]
Ω	0.467	0.380	0.452	0.406

specimen (b) in Fig. 1, the residual fatigue life of the [335] crystal was measured.

Fig. 2a and b shows the fatigue life curves of the GB, [123] and [335] crystals in the [123]/[335] bicrystal. It can be seen that the fatigue life in the [123]/[335] bicrystal increases in the order of GB, [123] and [335] crystals under the same cyclic tension-tension load. When the [123]/[335] and [5 9 13]/[579] bicrystal specimens of Fig. 1c were applied to cyclic push-pull straining, similar to that under cyclic tension-tension loading of the [123]/[335] bicrystal, the GBs were always the preferential failure sites. Meanwhile, it can be seen that there is a significant difference in the GB fatigue lives between [123]/[335] and [5 9 13]/[579] bicrystals, as shown in Fig. 2c. The average GB life of the [5 9 13]/[579] bicrystal is approximately 2–3 times higher than that of the [123]/[335] bicrystal.

From the results above, it is noted that there exists a distinct difference in the fatigue lives between GBs and the component crystals. Regardless of the GB structure of the bicrystals, the difference in the fatigue lives can be partially attributed to the effect of the component crystal orientations. First, the Schmid factors of primary slip systems of the four component crystals were calculated, and the results are listed in Table 1. It is apparent that the Schmid factors of primary slip systems in those component crystals increase in the following order:

$$\Omega_{[335]} < \Omega_{[579]} < \Omega_{[5\ 9\ 13]} < \Omega_{[123]} \quad (1)$$

For the [123]/[335] bicrystal specimen (Fig. 1b), the resolved shear stresses $\tau_{[123]}$ and $\tau_{[335]}$ applied on the primary slip systems of the [123] and [335] component crystals should be different when applying the same load P , i. e.

$$P\Omega_{[123]}/A_{[123]} = \tau_{[123]} > \tau_{[335]} = P\Omega_{[335]}/A_{[335]} \quad (2)$$

Here, $A_{[123]}$ and $A_{[335]}$ are the section areas the [123] and [335] component crystals. Therefore, under the same tension-tension load P , the plastic strain $\epsilon_{[123]}$ carried by the [123] crystal would be larger than $\epsilon_{[335]}$ carried by the [335] crystal in the [123]/[335] bicrystal specimen, i. e.

$$\epsilon_{[123]} > \epsilon_{[335]} \quad (3)$$

This will make the area $A_{[123]}$ of the [123] crystal to be smaller than $A_{[335]}$ of the [335] crystal during cyclic deformation. As a result, the stress applied on the [123] crystal will be further increased. It is natural that the [123] crystal always displayed lower fatigue life than the [335] crystal under the same cyclic load (Fig. 2a).

When [123]/[335] and [5 9 13]/[579] bicrystal specimens were cycled under push-pull straining, it was observed that their original areas changed little because the applied plastic strain range was relatively low (below 10^{-3} , as shown in Fig. 2c). Therefore, for each bicrystal, the average axis stresses of the two component crystals should be identical. However, the resolved shear stresses on the primary slip systems are not the same owing to the difference in orientations of the component crystals. Previously, it has been ob-

served that the softer [149] crystal with a higher Schmid factor always carried more plastic strain than the harder [001] crystal with lower Schmid factor in a [001]/[149] Cu bicrystal [12]. Similar to the result in the [001]/[149] bicrystal, when [123]/[335] and [5 9 13]/[579] bicrystals were applied to the same plastic strain, it can be concluded from Eq. (1) that the plastic strain carried by the four component crystals should decrease in the following order:

$$\epsilon_{[123]} > \epsilon_{[5\ 9\ 13]} > \epsilon_{[579]} > \epsilon_{[335]} \quad (4)$$

Thus, we can get

$$\epsilon_{[123]} - \epsilon_{[335]} > \epsilon_{[5\ 9\ 13]} - \epsilon_{[579]} \quad (5)$$

Since the plastic strain carried by each component crystal is different, there should be a strain gradient across the GB in the whole section of bicrystals. From Eq. (5), it can be concluded that the plastic strain gradient across the GB of the [123]/[335] bicrystal should be higher than that of the [5 9 13]/[579] bicrystal. This might be one of the reasons why the fatigue life of [123]/[335] bicrystals was always lower than that of [5 9 13]/[579] bicrystals under constant strain control, regardless of GB structure of the two bicrystals.

3.2 Fatigue damage and cracking mechanisms

It has been observed that fatigue crack always nucleated and propagated along the GB in the [123]/[335] Cu bicrystal, no matter whether under cyclic tension-tension loading or push-pull strain cycling. Fig. 3a shows a typical intergranular fatigue crack in the [123]/[335] bicrystal. With further cyclic deformation, the intergranular crack would propagate along the GB plane gradually and lead to final failure of the bicrystal. For the [5 9 13]/[579] bicrystal, it was also observed that the GB was still the preferential site for fatigue cracking under push-pull strain cycling, as shown in Fig. 3b, and in the end, intergranular fracture would take

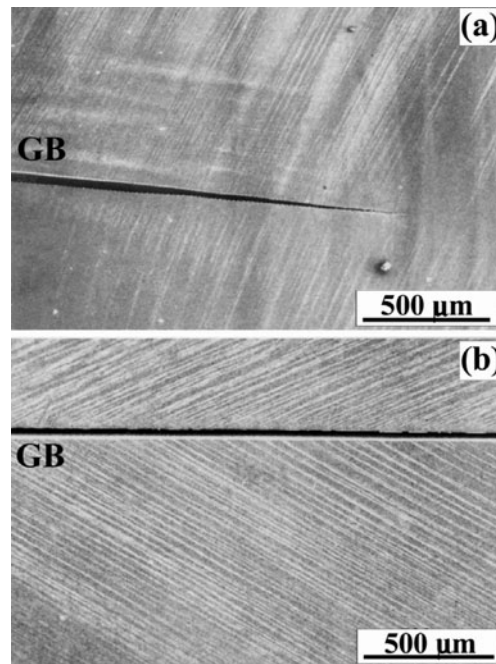


Fig. 3. Intergranular fatigue cracking in (a) [123]/[335] and (b) [5 9 13]/[579] bicrystals.

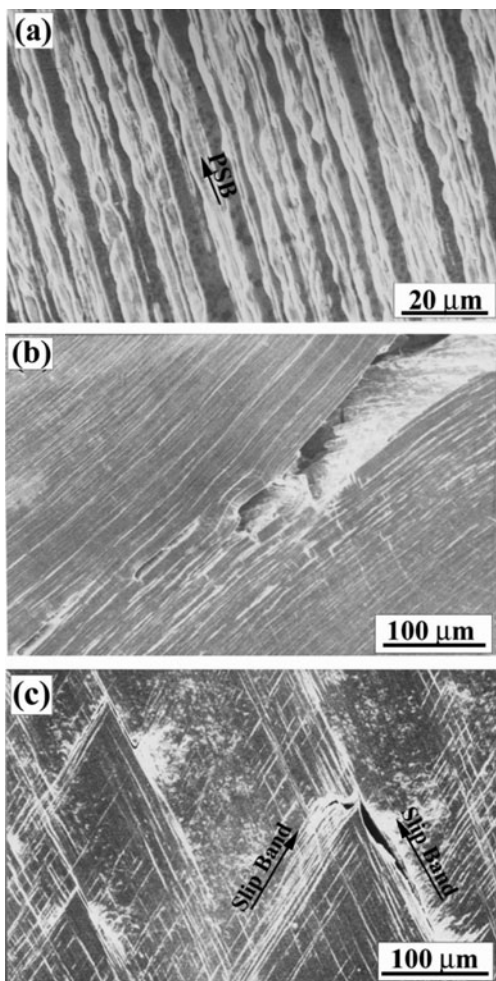


Fig. 4. (a) Fatigue damage on the component crystal surface induced by PSBs, (b) fatigue cracking on the surfaces of [123], and (c) [335] component crystals in a [123]/[335] Cu bicrystal under cyclic tension-tension loading.

place. The present results are in good agreement with the observations in [345]/[117], [134]/[134], [001]/[149] and [149]/[149] Cu bicrystals with a perpendicular GB [12–15]. This indicates that fatigue cracking along GBs in various bicrystals is a common phenomenon. These results further

proved that although the GBs often possess a higher strength than the component crystals under tension load, they are still the preferential sites for the nucleation and propagation of a fatigue crack under cyclic deformation condition.

Except for the intergranular fatigue cracking of the bicrystals, the component crystals were also damaged after cyclic deformation. The observations on the two crystal surfaces of the [123]/[335] bicrystal with reduced areas showed that the fatigue cracking was mainly induced by the surface slip bands. However, the modes of fatigue cracking in detail between [123] and [335] component crystals are distinctly different. For the [123] component crystal, as shown in Fig. 4a, there are many PSBs on the surface during cyclic deformation of the [123]/[335] bicrystal. With further cyclic deformation, these PSBs would become the preferential sites for fatigue cracking and led to transgranular fracture, as shown in Fig. 4b. The PSB cracking mechanism is in consistent with that in fatigued Cu single crystals [30–32]. For the [335] component crystal, however, fatigue cracking was found to mainly originate from the intersections between primary and secondary slip bands owing to the strain incompatibility, as shown in Fig. 4c. To date, fatigue crack initiation of the crystals with double-slip orientation has seldom been reported. The present study provided a new observation on the fatigue cracking of the double-slip-oriented [335] crystals. Therefore, the orientations of the crystals play a decisive role in the fatigue cracking mechanisms and furthermore affect their fatigue life, see the results in Fig. 2a.

For pure face-centered cubic single crystals, it was observed that fatigue crack initiation is always associated with the formation of PSBs, which carried out most of plastic strain during cyclic deformation [27, 28]. The PSB damage mechanism during cyclic deformation was often explained as the surface roughness caused by slip irreversibility (Fig. 4a). Concerning the GB damage mechanism, Kim and Laird [4] had proposed a step mechanism for intergranular cracking in Cu polycrystals fatigued at high strain amplitude. Afterwards, Mugrabi et al. [5] and Liu et al. [8] attributed the intergranular cracking to piling-up of PSBs at the GB and defined this process as the PSB-GB damage mechanism. Since most of the plastic strain is carried by PSBs

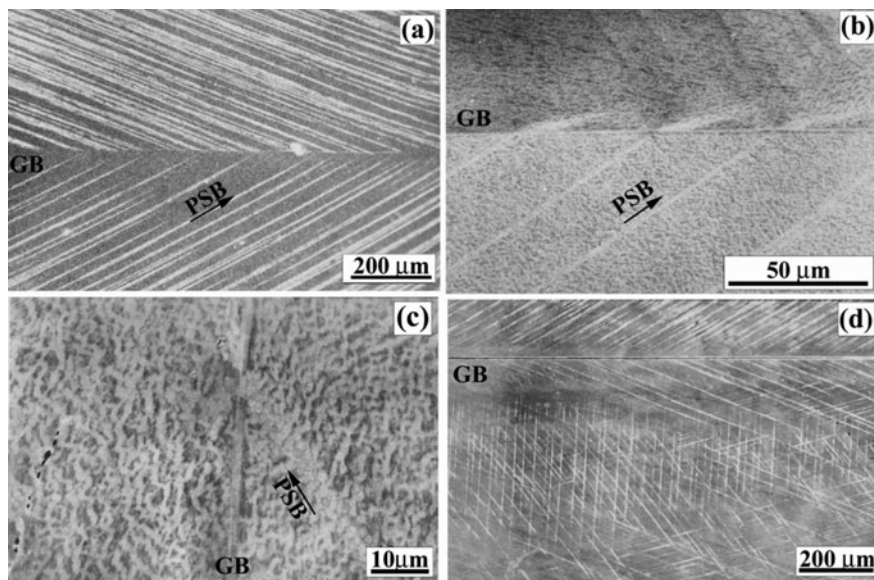


Fig. 5. (a) Interactions of surface PSBs with the GB in a [5913]/[579] bicrystal. (b, c) Dislocation patterns near the GB in [5913]/[579] bicrystals observed by the SEM-ECC technique. (d) Interactions of PSBs with the GB in a [123]/[335] bicrystal.

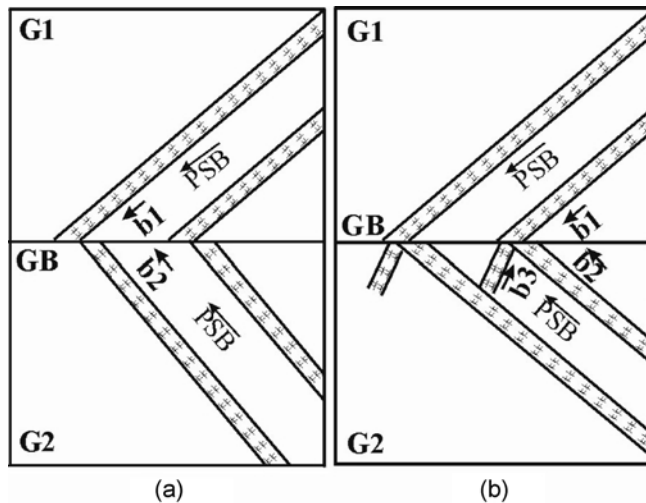


Fig. 6. Illustration of interactions between PSBs and GBs in (a) a [5913]/[579] bicrystal and (b) a [123]/[335] bicrystal.

and many defects (including dislocations and vacancies) are produced during cyclic plastic deformation of metallic materials. PSB may become a carrier or channel transporting residual dislocations (or vacancies) from the interior of grains to the GBs according to the PSB-GB cracking mechanism. For the [5 9 13]/[579] Cu bicrystal, the interactions of PSBs with GB had attracted much more attention in our previous work [20]. By the SEM-ECC technique, the slip morphology and dislocation patterns near a GB can be clearly observed, as shown in Figs. 5a–c. It can be seen that the surface PSBs beside a GB cannot transfer through and will be terminated at the GB (Fig. 5a). Dislocation pattern observations near the GB also showed that the dislocation carried by the PSBs cannot pass through the GB (Figs. 5b and c). Therefore, the interaction of PSBs (or dislocations) with the GB in the [5 9 13]/[579] bicrystal can be simply illustrated in Fig. 6a. For the [123]/[335] bicrystal, secondary slip bands were observed to be activated near the GB, as shown in Fig. 5d. Therefore, the interactions of PSBs with the GB in the [123]/[335] bicrystal can be illustrated in Fig. 6b. Obviously, in the two bicrystals, dislocation piling-up at the GB will always exist no matter whether the secondary slip bands were activated or not, as illustrated in Figs. 6a and b. With further cyclic deformation, when the dislocation piling-up at the GB was accumulated to an high enough density, intergranular fatigue cracking will occur along the GB under external stress. We can define this process as “piling-up of defects”, which is consistent with the PSB-GB damage mechanism [5, 6]. Essentially, intergranular fatigue cracking should be attributed to the accumulation of dislocations and vacancies at GBs. However, under unidirectional loading, dislocations and vacancies piled-up at a GB cannot be accumulated to high enough in density. Consequently, it is natural that the GB is a weaker element than the component crystals under cyclic loading, even though it is always stronger than the component crystals under tensile deformation.

3.3 Fatigue fractography observations

Fig. 7a shows a typical fatigue fractograph of a [123]/[335] bicrystal sample according to Fig. 1c under cyclic push-pull straining. It can be seen that there existed many fatigue striations which are very similar to the observations in

fatigued polycrystalline materials. For the [5 9 13]/[579] bicrystal, its fatigue fractography did not show an obvious difference from that of the [123]/[335] bicrystal. The fatigue striations can be attributed to the closure of the fatigue crack induced by the compressive cycling during the cyclic push-pull straining. Under the cyclic tension-tension loading of the [123]/[335] bicrystal, it was found that the fractured surface along the GB plane is relatively smooth at lower magnification (Fig. 7b). At higher magnification, some regular steps can be clearly observed in detail as marked by arrows (Fig. 7c). This feature is distinctly different from the fatigue striations on the fracture induced by cyclic push-pull cycling. Herein, we define them as slip steps induced by the PSBs. As we know, the interaction of PSBs with GBs often led to intergranular fracture and was defined as the PSB-GB damage mechanism. Under cyclic tension-tension cycling, the interactions of PSBs with a GB would be well maintained and may appear in the form of fine and regular slip steps on the fatigue fractographs (Figs. 8a and b). Essentially, those fine slip steps on the fractographs should be induced by the impingement of PSBs to the GB during cyclic tension-tension loading.

In our recent work, the PSB-GB cracking mechanism was also employed to explain the GB cracking phenomenon in Cu bicrystals with GBs parallel, perpendicular and tilted

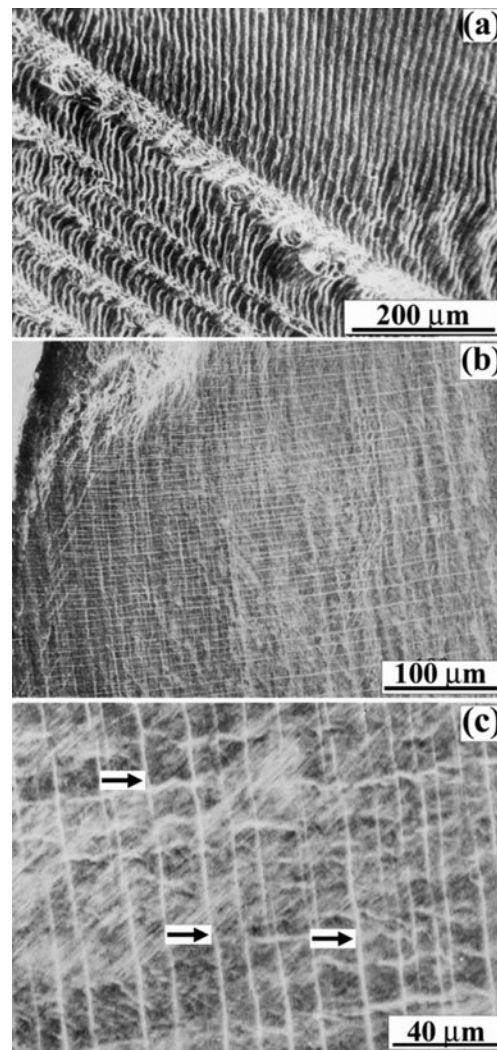


Fig. 7. Fatigue fractographs of a [123]/[335] bicrystal (a) under cyclic push-pull loading and (b, c) under cyclic tension-tension loading.

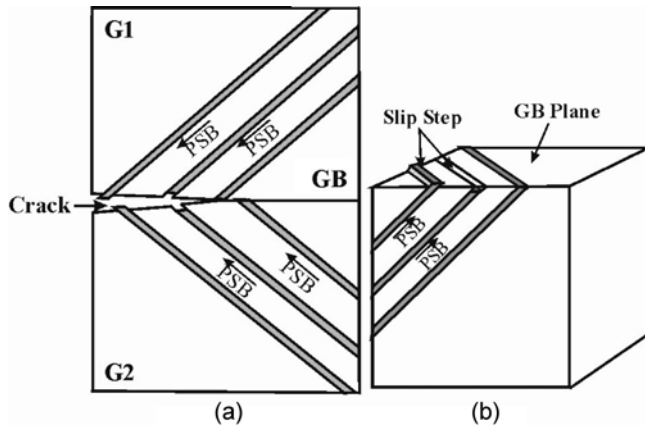


Fig. 8. Illustration of the interactions of PSBs with a GB in a [123]/[335] bicrystal under cyclic tension-tension loading, showing the formation of slip steps on the fatigue fractograph.

to the stress axis [12–19]; however, evidence by fatigue fractography was not provided. Therefore, the present result can be regarded as a new evidence to strengthen the PSB-GB damage mechanism. Although the GB structure and the component crystals are identical in the [123]/[335] bicrystals during cyclic tension-tension and push-pull cycling, their fatigue fractographs displayed a distinct difference (Figs. 7a–c). It is considered that the difference in fatigue fractography of the [123]/[335] bicrystals can be attributed to the difference in the testing conditions.

4 Conclusions

1. Under cyclic tension-tension loading, fatigue fracture always occurred along the GB of [123]/[335] Cu bicrystals with a uniform section area. When the section area of the GB segment is larger than that of the component crystals, the softer [123] crystal always showed a shorter fatigue life than the harder [335] crystal under the same cyclic load, indicating that the fatigue lives of the component crystals depend on their orientations. It is suggested that the fatigue lives increase in the order of GB, [123] and [335] crystals in [123]/[335] bicrystal.
2. Under cyclic tension-tension loading or push-pull straining, the GBs in [123]/[335] and [5913]/[579] Cu bicrystals were still the preferential sites to fatigue crack initiation and propagation. However, the fatigue life of the [5913]/[579] bicrystal is approximately 2–3 times higher than that of the [123]/[335] bicrystal, which was attributed to the difference in the orientations of their component crystals.
3. SEM observations showed that transgranular fatigue fracture of [123]/[335] Cu bicrystals with a reduced section area could be induced by cracking either along PSBs of the [123] crystal or the intersection of primary and secondary slip bands of the [335] crystal.
4. SEM-ECC observations revealed that the dislocations carried by PSBs could not pass through the GBs and were piled-up at the GBs, which resulted in the fatigue cracking of the Cu bicrystals during cyclic deformation. Essentially, it is proposed that the accumulation of dislocations or vacancies at the GB should be responsible

for intergranular cracking. Therefore, the GB is a weaker element than the component crystals during cyclic loading, even though it is always stronger than the component crystals under tensile deformation.

5. Fatigue fractography of [123]/[335] Cu bicrystal displayed two typical features: Fatigue striations induced by push-pull strain cycling and slip steps induced by cyclic tension-tension loading, which is suggested to be a new evidence for the PSB-GB damage mechanism.

This work was financially supported by the Special Funding for the National 100 Excellent Ph. D. Thesis provided by the Chinese Academy of Sciences. One of the authors (Z. F. Z.) wishes to acknowledge the Alexander von Humboldt Foundation for providing a postdoctoral fellowship.

References

1. Watanabe, T.: Mater. Forum 11 (1988) 284.
2. Aust, K.; Erb, U.; Palumbo, G.: Mater. Sci. Eng. A176 (1994) 329.
3. Randle, V.: Acta Mater. 46 (1998) 1459.
4. Kim, H.; Laird, C.: Acta Metall. 26 (1978) 787.
5. Mughrabi, H.; Wang, R.; Differt, K.; Essmann, U.: ASTM STP 811 (1983) 5.
6. Lim, L.C.; Acta Metall. 35 (1987) 1653.
7. Christ, H.-J.: Mater. Sci. Eng. A 117 (1989) 25.
8. Liu, W.; Bayerlein, M.; Mughrabi, H.; Day, A.; Quedstedt, P.N.: Acta Metall. Mater. 40 (1992) 1653.
9. Huang, H.L.; Ho, N.J.: Mater. Sci. Eng. A 293 (2001) 7.
10. Richter, R.; Burmeister, H.-J.: Acta Mater. 45 (1997) 715.
11. Him, G.-H.; Kwon, I.-B.: Mater. Sci. Eng. A 142 (1991) 177.
12. Peralta, P.; Laird, C.: Acta Mater. 45 (1997) 3029.
13. Hu, Y. M.; Wang, Z.G.: Scripta Mater. 35 (1996) 1019.
14. Hu, Y. M.; Wang, Z.G.: Int. J. Fatigue 19 (1997) 59.
15. Hu, Y. M.; Wang, Z.G.: Int. J. Fatigue 20 (1998) 463.
16. Zhang, Z.F.; Wang, Z.G.; Li, S.X.: Fatigue Fract. Eng. Mater. Struct. 17 (1998) 1307.
17. Zhang, Z.F.; Wang, Z.G.; Hu, Y.M.: Mater. Sci. Eng. A 269 (1999) 136.
18. Zhang, Z.F.; Wang, Z.G.; Hu, Y.M.: Mater. Sci. Eng. A 272 (1999) 410.
19. Zhang, Z.F.; Wang, Z.G.: Phil. Mag. Lett. A 80 (2000) 483.
20. Zhang, Z.F.; Wang, Z.G.: Phil. Mag. A 79 (1999) 741.
21. Zauter, R.; Petry, F.; Bayerlein, M.; Sommer, C.; Christ, H.-J.; Mughrabi, H.: Phil. Mag. A 66 (1992) 425.
22. Wilkinson, A.J.; Hirsch, P.B.: Phil. Mag. A74 (1995) 81.
23. Wilkinson, A.J.; Henderson, M.B.; Martin, J.W.: Phil. Mag. Lett. 74 (1996) 145.
24. Bretschneider, J.; Holste, C.; Tippelt, B.: Acta Mater. 45 (1997) 3755.
25. Zhang, Z.F.; Wang, Z.G.: Acta Mater. 46 (1998) 5063.
26. Zhang, Z.F.; Wang, Z.G.; Su, H.H.: Phil. Mag. Lett. 79 (1999) 233.
27. Zhang, Z.F.; Wang, Z.G.; Li, S.X.: Phil. Mag. Lett. 80 (2000) 525.
28. Zhang, Z.F.; Wang, Z.G.; Sun, Z.M.: Acta Mater. 49 (2001) 2875.
29. Jia, W.P.; Li, S.X.; Wang, Z.G.; Li, X.W.; Li, G.Y.: Acta Mater. 47 (1999) 2165.
30. Essmann, U.; Gösele, U.; Mughrabi, H.: Phil. Mag. A 44 (1981) 406.
31. Hunsche, A.; Neumann, P.: Acta Metall. 34 (1986) 207.
32. Ma, B.-T.; Laird, C.: Acta Metall. Mater. 37 (1989) 325.

(Received March 25, 2002)

Correspondence address

Dr. Z. F. Zhang
 Institute for Metallic Materials
 P. O. 270016, D-01171 Dresden, Germany
 Tel: +49 351 465 9766
 Fax: +49 351 465 9541
 E-mail: z.f.zhang@ifw-dresden.de